Numerical Analysis of Hot Water Layer Formation in Pool Type Research Reactor

Yong-Seok Choi[1*], Hyun-Gi Yoon[2], and Kyoung-Woo Seo[2]
[1]Reactor System Safety Research Division, [2]Research Reactor System Design Division,
Korea Atomic Energy Research Institute, Daejeon, Korea
[*]Corresponding author: cys@kaeri.re.kr

1. Introduction

The effectiveness of the hot water layer on the radiation level of the pool-top has been investigated in several studies [1-3]. In HANARO, the hot water layer system (HWLS) was additionally implemented to the fluid system to solve the pool top radiation problem originated from the highly activated core bypass flow [1]. After implementing the system, the activity of major nuclides dissolved in the pool water such as ^{24}Na was sufficiently reduced in the hot water layer region. The role of HWLS is also studied for radioprotection in the Egyptian research reactor, ETRR-2 [2]. They calculated dose rate using conventional code and predicted the radiation dose rate above the pool surface. The effectiveness of the hot water layer was also confirmed by measuring the dose rate above the ETRR-2 pool [3]. It was decreased as the temperature difference between the hot water layer and the mean pool water exceeds by 4℃. On the other hand, the hot water layer of the RMB research reactor project in Brazil was numerically analyzed using a commercial code [4]. But the flow fields inside the reactor structure and fuel assembly were analyzed rather than the hot water layer itself.

In this paper, formation of thermal stratification in an initially quiescent pool of JRTR (Jordan Research and Training Reactor) is analyzed by using a commercial code, ANSYS FLUENT13. For the treatments of Reynolds stresses and turbulent heat fluxes, the two-equation realizable k-ε model and the simple gradient diffusion hypothesis (SGDH) are used since the present study is focus on an industrial scale evaluation. We emphasize the assumptions and numerical methods used in the calculation. The validity of the numerical methods is discussed with the measured data obtained during the system commissioning. Suggestions for the model improvement are finally given as a concluding remark.

2. Description of Hot Water Layer System

The HWLS consists essentially of a pump, an ion-exchanger, and a heater, which are arranged in a serial order as shown in Fig. 1. The pump provides necessary head for the flow rate of 2.5 kg/s and the electric heater has 100 kWt capacity. The ion-exchanger, which is indifferent to the hot water layer formation, removes ionic radioactive impurities transported to the hot water layer to reduce the pool top radiation level as low as achievable.

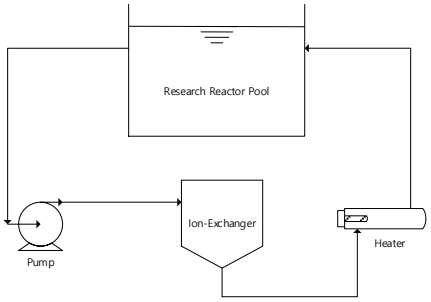

Fig. 1. Flow diagram of hot water layer system

3. Mathematical Formulations

3.1 Governing equations

The governing equations for the conservation of mass, momentum, and energy in ensemble-averaged form can be written as follows;

$$\frac{\partial \rho}{\partial t}+\frac{\partial}{\partial x_i}(\rho u_i)=0 \tag{1}$$

$$\frac{\partial}{\partial t}(\rho u_i)+\frac{\partial}{\partial x_j}(\rho u_i u_j)= -\frac{\partial p}{\partial x_i}+\frac{\partial}{\partial x_j}\left[\mu\left(\frac{\partial u_i}{\partial x_j}+\frac{\partial u_j}{\partial x_i}\right)-\rho\overline{u_i' u_j'}\right]-\rho g_i\beta\left(T-T_{ref}\right) \tag{2}$$

$$\frac{\partial}{\partial t}(\rho T)+\frac{\partial}{\partial x_i}[\rho T u_i]=\frac{\partial}{\partial x_j}\left[\frac{\mu}{\mathrm{Pr}}\frac{\partial T}{\partial x_j}-\rho\overline{\theta u_j}\right] \tag{3}$$

where $-\rho\overline{u_i' u_j'}$ are the Reynolds stresses and $-\rho\overline{\theta u_j}$ are the turbulent heat fluxes. In the momentum equation, the Boussinesq approximation is adopted to reflect the buoyancy force term. The Reynolds stresses and the turbulent heat fluxes should be computed using appropriate turbulence modeling.

3.2 Turbulence model

The realizable *k-ε* model is employed in the present study for the turbulence model [5]. This model satisfies certain mathematical constraints on the Reynolds stresses, consistent with the physics of turbulent flows. In this turbulence model, the Reynolds stresses are modeled employing the Boussinesq hypothesis to relate them to the mean velocity gradient as follow [6];

$$-\rho\overline{u_i' u_j'}=\mu_t\left(\frac{\partial u_i}{\partial x_j}+\frac{\partial u_j}{\partial x_i}\right)-\frac{2}{3}\rho k\delta_{ij} \tag{4}$$

where μ_t is the eddy viscosity which is defined as;

$$\mu_t = \rho C_\mu \frac{k^2}{\varepsilon} \tag{5}$$

In the realizable k-ε model, C_μ is a function of the mean strain and rotation rates which is computed from;

$$C_\mu = \frac{1}{A_0 + A_S \frac{kU^*}{\varepsilon}} \tag{6}$$

where

$$U^* = \sqrt{S_{ij}S_{ij} + \Omega_{ij}\Omega_{ij}}, \quad S_{ij} = \frac{1}{2}\left(\frac{\partial u_j}{\partial x_i} + \frac{\partial u_i}{\partial x_j}\right), \ \Omega_{ij} = \frac{1}{2}\left(\frac{\partial u_j}{\partial x_i} - \frac{\partial u_i}{\partial x_j}\right) \tag{7}$$

The model constants for the equation (6) are given by;

$$A_0 = 4.04, \ A_S = \sqrt{6}\cos\varphi \tag{8}$$

where

$$\varphi = \frac{1}{3}\cos^{-1}\left(\sqrt{6}W\right), \ W = \frac{S_{ij}S_{jk}S_{ki}}{\tilde{S}^3}, \ \tilde{S} = \sqrt{S_{ij}S_{ij}} \tag{9}$$

In ANSYS FLUENT, the turbulent heat transport of equation (3) is modeled using the concept of Reynolds' analogy to turbulent momentum transfer as follow;

$$\frac{\partial}{\partial t}(\rho E) + \frac{\partial}{\partial x_i}\left[u_i(\rho E + p)\right] = \frac{\partial}{\partial x_j}\left[k_{eff}\frac{\partial T}{\partial x_j}\right] \tag{10}$$

where E is the total energy and k_{eff} is the effective thermal conductivity which is defined as;

$$k_{eff} = k + \frac{c_p \mu_t}{Pr_t} \tag{11}$$

where k is the thermal conductivity, c_p is the heat capacity at constant pressure, and Pr_t is the turbulent Prandtl number of 0.85. Therefore the turbulent heat fluxes in equation (3) are modeled by the SGDH as;

$$-\rho\overline{\theta u_j} = \frac{\mu_t}{Pr_t}\left(\frac{\partial T}{\partial x_j}\right) \tag{12}$$

The transport equations for k and ε in the realizable k-ε model are as follows;

$$\frac{\partial}{\partial t}(\rho k) + \frac{\partial}{\partial x_j}(\rho k u_j) = \frac{\partial}{\partial x_j}\left[\left(\mu + \frac{\mu_t}{\sigma_k}\right)\frac{\partial k}{\partial x_j}\right] + G_k + G_b - \rho\varepsilon \tag{13}$$

$$\frac{\partial}{\partial t}(\rho \varepsilon) + \frac{\partial}{\partial x_j}(\rho \varepsilon u_j) = \frac{\partial}{\partial x_j}\left[\left(\mu + \frac{\mu_t}{\sigma_\varepsilon}\right)\frac{\partial \varepsilon}{\partial x_j}\right] + \rho C_1 S\varepsilon - \rho C_2 \frac{\varepsilon^2}{k + \sqrt{\nu\varepsilon}} \tag{14}$$

where

$$C_1 = \max\left[0.43, \frac{\eta}{\eta + 5}\right], \ \eta = S\frac{k}{\varepsilon}, \ S = \sqrt{2S_{ij}S_{ij}} \tag{15}$$

In these equations, G_k is the generation of turbulence kinetic energy due to the mean velocity gradients, G_b is the generation of turbulence kinetic energy due to buoyancy, C_2 is a constant, σ_k and σ_ε are the turbulent Prandtl numbers for k and ε, respectively. The model constants are as follows;

$$C_2 = 1.9, \ \sigma_k = 1.0, \ \sigma_\varepsilon = 1.2 \tag{16}$$

The term G_k is defined as;

$$G_k = -\rho\overline{u_i' u_j'}\frac{\partial u_j}{\partial x_i} = \mu_t S^2 \tag{17}$$

and the term G_b is given by;

$$G_b = \beta g_i \frac{\mu_t}{Pr_t}\frac{\partial T}{\partial x_i} \tag{18}$$

Equation (18) indicates that the turbulence kinetic energy, k, tends to be produced in unstable stratification and to be suppressed in stable stratification.

4. Boundary Conditions

4.1 Heat losses

Upon the formation of the hot water layer, heat loss to the surrounding is unavoidable due to the following inherent heat transfer mechanisms. (a) Evaporation from the pool surface, (b) air convection above the pool surface, (c) conduction through the reactor wall, (d) heat losses from the piping and the components of the HWLS, (e) heat transfer from the hot water layer to the lower part of the pool. Among these heat losses, (c) is assumed to be negligible because the pool water is confined in a pool liner which is shortly apart from the concrete wall. (d) is also neglected since thermal insulations are applied on the piping and the components.

Heat loss by the evaporation is modeled using an empirical equation [7].

$$w_p = A(p_w - p_a)(0.089 + 0.0782V)/Y \tag{19}$$

where, w_p, evaporation rates; A, pool area; Y, latent heat; p_w, saturation vapor pressure at surface water temperature; p_a, saturation pressure at room air dew point; V, air velocity. Therefore the unit heat loss by evaporation, q_{evap}, can be estimated by following equation.

$$q_{evap} = w_p Y / A \tag{20}$$

The pool area is 38.5 m^2, p_a is 0.659 kPa, and V is 0.055 m/s from the design parameters of the JRTR.

Heat loss by the convection above the pool surface is modeled using an empirical equation [8].

$$\overline{Nu} = 0.15 Ra_L^{1/3} \ (10^7 \le Ra_L \le 10^{11}), \quad Ra_L = g\beta(T_w - T_a)L^3/\nu\alpha \tag{21}$$

where, g, acceleration of gravity; β, thermal expansion coefficient, L, characteristic length; ν, dynamic viscosity, α, thermal diffusivity. The above properties should be taken from the film temperature, mean of surface water and room air temperatures. Finally the unit heat loss by the convection of air is estimated as,

$$q_{conv} = h(T_w - T_a) \tag{22}$$

4.2 Discharge temperature

As the heater operates, the pool temperature gradually rises and the heater inlet temperature also increases. Since the PID (proportional integral

derivation) control of the heater automatically adjust the heater operating power, the heater runs in its full power until the heater outlet temperature reaches to a preset value. Then the PID control reduces the heater power accordingly to maintain the outlet temperature and finally a steady operation state is achieved. In the CFD model, the discharge temperature into the hot water layer is modeled as following.

$$\begin{aligned} T &= T_{intake} + Q_{heater} \big/ \dot{m} C_p \\ T_{discharge} &= T; \quad \text{where, } T < T_{preset} \\ T_{discharge} &= T_{preset}; \quad \text{where, } T \geq T_{preset} \end{aligned} \tag{23}$$

where, Q_{heater} = 100 kW; $\dot{m}$ = 2.5 kg/s; C_p = 4.183 kJ/kg-K; T_{preset} = 55℃. The specific heat of the water is regarded as constant since its variations are negligible in the calculated temperature ranges.

4.3 Other conditions

The shear stress on the pool surface is set to zero since it is a free surface. Except the pool surface, no-slip condition is applied on the wall boundary. Mass flow rate condition is set on the main inlet pipe. The flow is distributed in the T-shape distributor and discharged into the pool through evenly spaced discharge holes.

5. Numerical Methods

The geometry and grids are produced by the Geometry and the Mesh in the ANSYS Workbench 13.0. The patch conforming tetrahedrons method and the multi-zone method are used for the mesh generation. The tetrahedrons mesh is adopted for the hot water layer region and the multi-zone method is adopted below the hot water layer where the thermal stratification develops. Mesh sizing functions which consider the proximity and curvature of the geometry is used. The minimum and maximum cell sizes are restricted to 0.003 m and 0.1 m, respectively. Number of generated mesh cells is about 1.8 million. The calculation is done using a transient solver. Realized k-e model is adopted for the turbulence model. For the pressure-velocity coupling, SIMPLE scheme is adopted with the spatial discretization of second order upwind for momentum, turbulence, and energy.

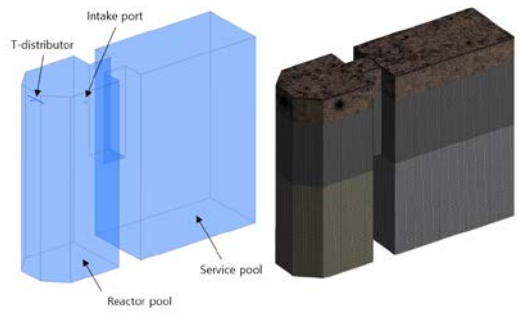

Fig. 2. Geometry and grids for the numerical analysis.

6. Results and Discussions

Fig. 3 shows a time history of the measured and calculated temperatures at the HWLS discharge and the suction. Although the calculated temperature histories show quite good agreement with the measured values, there exists a deviation for the suction temperatures. The calculation estimates quite higher temperature than the measurement. This seems to originate from the turbulence model for the calculation. It suggests that the realizable *k-ε* model underestimates the heat transfer through the thermally stratified region below the hot water layer.

Fig. 4 shows depth-wise temperature distribution in the reactor pool. The symbols indicate measured values and the solid lines are from the calculations. Process of hot water layer formation is remarkable according to the time. The calculation quite well simulates the actual phenomena including thickness of the hot water layer. However the calculated temperature is about 3 ℃ higher when development of the hot water layer reaches to quasi steady-state. This is due to the turbulence model as discussed in above paragraph. In Fig. 4 the calculations show stiff gradient then the measurement. This indicates that in real situation turbulence mixing is more prevail in the thermally stratified region than the prediction of the turbulence model.

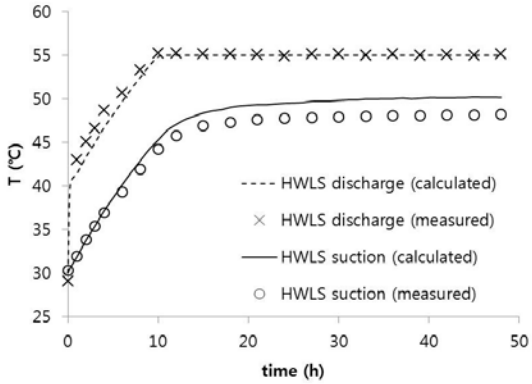

Fig. 3. Suction and discharge temperatures of the HWLS as a function of the time.

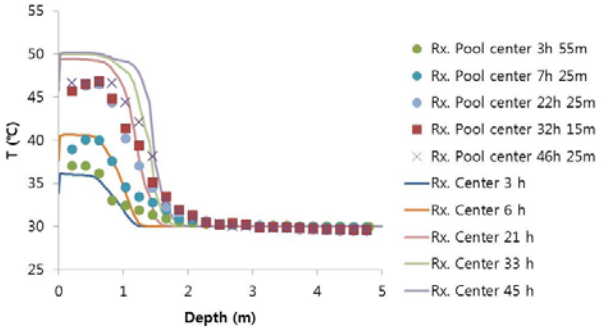

Fig. 4. Depth-wise temperature distribution in the reactor pool.

7. Conclusion

Formation of the hot water layer and the thermal stratification in a research reactor pool is analyzed using a commercial code. The two-equation realizable k-ε model and the SGDH are used for the treatments of Reynolds stresses and turbulent heat fluxes. Boundary conditions including the heat losses on the pool surface and the discharge temperature variation by heater operation are also considered. As results, the development of the hot water layer are successfully simulated. The calculation results are compared with the measured temperature and flow distribution data. Although there exists a small deviation between the measurement and the calculation, the present calculation method predicts the measured results acceptably.

Acknowledgement

This work was supported by the National Research Foundation of Korea (NRF) grant funded by the Korea government (MSIP) (No. NRF-2012M2C1A1026909).

REFERENCES

[1] C. S. Lee, S. J. Park, H. Kim, Y. C. Park, and Y. S. Choi, "Reduction of the pool-top radiation level in HANARO," Proceedings of the Sixth Asian Symposium on Research Reactors, Mar. 29-31, 1999, Mito, Japan, pp. 124-129.
[2] A. Abdelhady, "Radiological performance of hot water layer system in open pool type reactor," Alexandria Engineering Journal, Vol. 52, pp. 159-162, 2013.
[3] T. A. Elmaaty, "Experimental investigation of the hot water layer effect on upward flow open pool reactor operability," Arab Journal of Nuclear Science and Applications, Vol. 47, No. 3, pp. 7-15, 2014.
[4] L. Contreras, J., A. Doval, F. Francioni, P.E. Umbehaun, W.M. Torres, A. C. Prado and A. Belchior. Jr, 2014. Thermal-Hydraulic Aspects of RMB Design, 16th IGORR Conference.
[5] T.-H. Shih, W. W. Liou, A. Shabbir, Z. Yang, and J. Zhu, "A New k-ε Eddy-Viscosity Model for High Reynolds Number Turbulent Flows – Model Development and Validation," Computers Fluids, Vol. 24, No. 3, pp. 227-238, 1995.
[6] S.-K. Choi and S.-O Kim, "Turbulence modelling of natural convection in enclosures: A review," Journal of Mechanical Science and Technology, Vol. 26, No. 1, pp. 283-297, 2012.
[7] 2011 ASHRAE Handbook – Heating, Ventilating, and Air-Conditioning Applications, American Society of Heating, Refrigerating and Air-Conditioning Engineers, Inc., Atlanta, GA, 2011.
[8] Fundamentals of Heat and Mass Transfer 5th Edition, F. P. Incropera and D. P. DeWitt, John Wiley & Sons, Inc., New York, NY, 2002.